JCAMECH

Investigation on Instability of Rayleigh-Benard Convection Using Lattice Boltzmann Method with a Modified Boundary Condition

Mostafa Varmazyar [a,*]; Mohammadreza habibi [b]; Arash Mohammadi [a]

[a] Department of Mechanical Engineering, Shahid Rajaee Teacher Training University, Tehran, Iran
[b] Research Institute of Petroleum Industry, Tehran, Iran

ARTICLE INFO

ABSTRACT

In this study, the effects of Prandtl number on the primary and secondary instability of the Rayleigh-Benard convection problem has been investigated using the lattice Boltzmann method. Two different cases as Pr=5.8 and 0.7 representing the fluid in liquid and gas conditions are examined. A body forces scheme of the lattice Boltzmann method was presented. Two types of boundary conditions in the presence of body forces are analyzed by the moment method and applied to a Poiseuille flow. Characteristic velocity was set in such a way that the compressibility effects are negligible. The calculations show that the increment of Prandtl number from 0.7 to 5.8 causes to create a secondary instability and onset of the oscillation in the flow field. Results show that at Pr=5.8, when the Rayleigh number is increased, a periodic solution appeared at Ra=48,000. It is observed that the dimensionless frequency ratio for Ra= 10^5 with Pr=5.8 is around 0.0065. The maximum Nusselt number for Ra = 10^5 with Pr=5.8 are estimated to be 5.4942.

1. Introduction

Natural convection has many applications in nature and industry. The massive fluid movements in the atmosphere [1] and oceans [2, 3], Polymerase chain reaction chip [4-6], cooling of microelectronic components, micro-structured devices, and Micro-Electro-Mechanical-System devices [7-13] are some common examples. Natural convection in many cases is explained in terms of the Rayleigh-Benard problem [14-16]. Rayleigh-Benard convection is a transport phenomenon which consists of a fluid subject to an external gravity field placed between two horizontal plates, heated from below and cooled from above.

There is no exact solution for the set of conservation equations describing a Rayleigh-Benard convection problem. Several numerical and experimental investigations have been made the onset of convection and the transition to pattern formation in Rayleigh-Benard with periodic temperature boundary condition [17-22]. The aforementioned numerical studies which investigate Rayleigh-Benard problem apply the conventional Computational Fluid Dynamics (CFD) to model the primary and secondary instability. Conventional CFD is based on continuum approach and direct discretization of momentum and energy conservation equations. These methods have a macroscopic view in dealing with fluid heat transfer and dynamics problems. Alternatively, the kinetic methods for CFD, such as the lattice Boltzmann method, take a microscopic approach and are derived from the Boltzmann equation [23-29]. In the solvers which are developed by lattice Boltzmann method, there is no need to use the pressure correction equation. Meantime, the lattice Boltzmann equation is a first-order equation on the space. These capabilities, as compared to the Navier Stokes equation, will increase the speed of solution and reduce the cost of the calculations.

Modeling of fluids under influence of body forces e.g. buoyancy driven flow [30-32] as well as magneto-hydrodynamic fluid flow [33, 34], multi-phase or multi-component fluid flows [35-38] and flow of non-ideal gases obeying a van der Waals type of equation of state [39-41] is a topic of interest in lattice Boltzmann research area. To simulate the buoyancy driven flows, a suitable scheme to model the buoyancy force, as well as the boundary conditions in the presence of the body forces, are needed to be introduced.

Shan [42] used the lattice Boltzmann model for investigating Rayleigh-Benard convection with one distribution function for the fluid flow simulation and another distribution function for modeling the thermal transport. Comparison between the results of Shan [42] and those of Clever and Busse [43] show that the Nusselt number values are in good agreement only for flows with Ra < 20000. He et al. [44] calculated the temperature by an internal energy distribution function, rather than a passive-scalar approach. Likewise, Shan [42], the results of He et al. [44] were in good agreement with Clever and Busse's [45] benchmark calculations for Ra < 20,000. Kao and Yang [46] used the lattice Boltzmann method to investigate about secondary instability in a Rayleigh–Benard problem where the Prandtl number is higher than 0.7. They reported that the mean value of the Nusselt number under the fluctuations due to the secondary instability

---

* Corresponding author. Tel.: +98-21-229-70063; fax: +98-21-229-70033;

e-mail: varmazyar.mostafa@sru.aci.ir

only depend on the Rayleigh number and is independent of Prandtl number. In addition, they have claimed that the mean value of the Nusselt number is equal to the value of the Nusset number when the oscillations are not observed in a specific Rayleigh number. Recently, Wang et al. [47] extensively investigated about the amount of Nusselt number under non-oscillating conditions. They showed that the value of the Nusselt number depends simultaneously on the Rayleigh and Prantel numbers. These results are not consistent with the results of Kao and Yang [46]. In order to clarify this inconsistency, the present study aims to investigate the value of the Nusselt number under oscillating conditions.

Kao and Yang [46] is used the simplest forms of body force simulation scheme and the bounce back method. To increase the accuracy of the lattice Boltzmann method in the presence of the buoyancy force term, more concentrations should be made on the boundary conditions. As mentioned in [48], the force and velocity equations are modified in order to model the effect of body forces. The boundary conditions also need to be adjusted accordingly. The most common set of boundary conditions used in the lattice Boltzmann method is the bounce-back model. In this type of boundary conditions, the particles bounce-back to the fluid nodes in opposite directions from which they strike the wall nodes. The set of boundary conditions may be categorized in terms of the order of magnitude of the error generated [49]. Many attempts have been made to introduce higher order schemes for boundary conditions [49-54]. The bounce-back approach satisfies the mass conservation on the wall and assures the zero velocity on the boundary. However, a problem appears once the body forces are present. Li and Tafti [55] showed that applying the common bounce-back boundary condition leads to an erroneous velocity jump at the wall in the presence of local forces due to static and dynamic forces. To eliminate the unwanted velocity component, they proposed a consistent mass conserving velocity-boundary condition for the D2Q9 lattice configuration in the presence of surface forces. Recently, Allen and Reis [56] used a general approach for executing lattice Boltzmann boundary conditions in terms of the moments of the distribution functions. This methodology, called 'moment method', was taken from Bennett [57] in which the wall is assumed to be located precisely at grid points. It means that this method stays completely local and does not need any extra finite difference schemes neither an interpolation nor extrapolation of magnitudes to or from adjacent nodes. In the present study, the Bennett methodology is employed to assess the Lie and Taftli [55] as well as the Allen and Reis [56] boundary conditions.

In next section, the governing equation based on lattice Boltzmann method has been described. Two physical models, Poiseuille and Rayleigh-Benard convection flow, have been investigated in results and discussion chapter.

2. Governing Equation and Modeling

The lattice Boltzmann method and corresponding thermal lattice Boltzmann method have been described below.

2.1. Lattice Boltzmann method

The lattice Boltzmann equation is directly derived from the Boltzmann equation by discretization in both time and phase space [24].The general form of the lattice Boltzmann equation in the ith direction with body forces included is:

$$f_i(\vec{r}+\vec{c}_i, t+1)-f_i(\vec{r},t)=\Omega_i+\tilde{F}_i \tag{1}$$

where $\vec{r}$, t and $\tilde{F}_i$ are the location vector, time and body forces respectively. The term f_i is the particle distribution function traveling with velocity $\vec{c}_i$. The collision operator Ω_i represents the rate of change of f_i due to collision of particles. The particle distribution after propagation is relaxed towards the equilibrium distribution $f_i^{eq}(\vec{r},t)$. The formulation of the Bhatnagar-Gross-Krook method (BGK) [58] for collision operator has been used in this study as:

$$\Omega_i = -\frac{1}{\tau}(f_i(\vec{r},t)-f_i^{eq}(\vec{r},t)) \tag{2}$$

The relaxation parameter τ has been calculated from the kinematic viscosity υ of the simulated fluid according to the following equation.

$$\tau = 3\upsilon + \frac{1}{2} \tag{3}$$

The equilibrium density $f_i^{eq}(\vec{r},t)$ is calculated as:

$$f_i^{eq}(\vec{r},t) = w_i\rho(\vec{r},t)\times$$
$$(1+\frac{\vec{c}_i.\vec{u}^{eq}}{c_s^2}+\frac{(\vec{c}_i.\vec{u}^{eq})^2}{2c_s^4}-\frac{\vec{u}^{eq}.\vec{u}^{eq}}{2c_s^2}) \tag{4}$$

where c_s is the speed of sound, and w_i is the corresponding equilibrium density for $\vec{u}^{eq}=0$. Taking the moment of the distribution function, the density and microscopic velocity may be obtained as follows.

$$\rho(\vec{r},t) = \sum_i f_i(\vec{r},t) \tag{5}$$

$$\vec{u}'(\vec{r},t) = \frac{1}{\rho(\vec{r},t)}\sum_i f_i(\vec{r},t)\vec{c}_i \tag{6}$$

The body force in the lattice Boltzmann model is calculated as below.

$$\vec{F} = (\rho - \rho_m)\vec{G} \tag{7}$$

where ρ_m and $\vec{G}$ are the average fluid density and gravity acceleration respectively. Using the Boussinesq approximation, the body force (buoyancy) term in Rayleigh-Benard convection will be

$$\vec{F} = -\rho\beta(T-T_m)\vec{G} \tag{8}$$

where T_m and β are the average fluid temperature and volumetric thermal expansion coefficients respectively.

2.2. Body Force Scheme

Guo et al. [48] assessed comprehensively the various methods introduced above by Chapmann-Enskog analysis. They recovered the Navier-Stokes equation from lattice Boltzmann method and introduced the extra terms associated with the error. They found that such extra terms can have a noticeable effect on lattice Boltzmann results in cases where the force term varies by time and in space. Therefore, they used the following generalized force term in a second order Hermit polynomials formulation that was first suggested by Ladd and Verberge [59] and Martys and Douglas [60] to exactly retrieve the macroscopic equation of Navier-Stokes.

$$
\tilde{F}_i = w_i \left[A + B \frac{\vec{c}_i . \vec{F}}{c_s^2} \right] +
$$
$$
w_i \left[C \frac{(\vec{u}^F \vec{F} + \vec{F} \vec{u}^F) : \left(\vec{c}_i . \vec{c}_i - c_s^2 I \right)}{2 c_s^4} \vec{c}_i \right] \tag{9}
$$

The study of Guo et al. [48], considered as Scheme of Guo, assumed the below velocity equations and found A, B and C equal to 0, $1 - 1/(2\tau)$ and $1 - 1/(2\tau)$, respectively.

$$
\vec{u}(\vec{r},t) = \vec{u}'(\vec{r},t) + \frac{\vec{F}(\vec{r},t)}{2\rho},
$$
$$
\vec{u}^{eq}(\vec{r},t) = \vec{u}'(\vec{r},t) + \frac{\vec{F}(\vec{r},t)}{2\rho},
$$
$$
\vec{u}^F(\vec{r},t) = \vec{u}'(\vec{r},t) + \frac{\vec{F}(\vec{r},t)}{2\rho} \tag{10}
$$

2.3. Thermal Lattice Boltzmann method

To simulate the energy equation the general form of the thermal lattice Boltzmann equation has been used. The equilibrium distribution function is considered as below.

$$
g_i^{eq}(\vec{r},t) = w_i \left(T + \frac{1}{c_s^2} \rho \vec{c}_i . \vec{u} \right) \tag{11}
$$

where T is the temperature. The relaxation time (λ) is related to the diffusion coefficient with equation 12.

$$
\lambda = \frac{1}{c_s^2} \alpha_0 + \frac{1}{2} \tag{12}
$$

where α_0 is the thermal diffusivity. The Temperature is calculated by equation 13.

$$
T = \sum_i g_i(\vec{r},t) \tag{13}
$$

2.4. Lattice Boltzmann method BC

For the Dirichlet boundary condition in thermal lattice Boltzmann method, it is assumed that the flux is balanced in any direction ($g_i - g_i^{eq} = g_j - g_j^{eq}$). The subscript i shows the

direction of particles after being reflected back to the domain. Subscript j shows the corresponding mirror direction of particles. For nodes on the wall, the balanced flux can be written as $g_i = (w_i + w_j)T_w - g_i^{eq}$ in which T_w is the wall temperature.

The introduced hydrodynamic boundary condition in this study is based on the Bennett extension. The moment-based model of Bennett [57] is a generalization of the method of Noble et al. [53] which formulates the boundary conditions in terms of the moments of the distribution functions, rather than on the distribution functions directly. In the moment-based approach, the nine independent moments can be defined as below.

$$
m = (\Pi_0, \Pi_X, \Pi_Y, \Pi_{XX}, \Pi_{YY}, \Pi_{XY},
$$
$$
\Pi_{XYY}, \Pi_{XXY}, \Pi_{XXYY}) \tag{14}
$$

where m may be expressed in the computational scale as $m = M \times f$ and M is a transform matrix defined as follows.

By this approach, the boundary condition method can be categorized. In the current study, the schemes of Li and Tafti [55] (BC-1) and Allen and Reis [56] (BC-2) are evaluated using the moment-based model of Bennett method. In both of BC-1 and BC-2 schemes, it is assumed that the solid boundaries are impermeable, rigid and stationary, and subjected to the no–slip condition. For calculating the three unknowns in each horizontal wall in terms of the moment constraints and the known distributions, it is required to consider three equations. The unknown values of f2, f5, and f6 pointing outwards with respect to the southern wall are to be calculated by using the after streaming values of f0, f1, f3, f4, f7, f8.
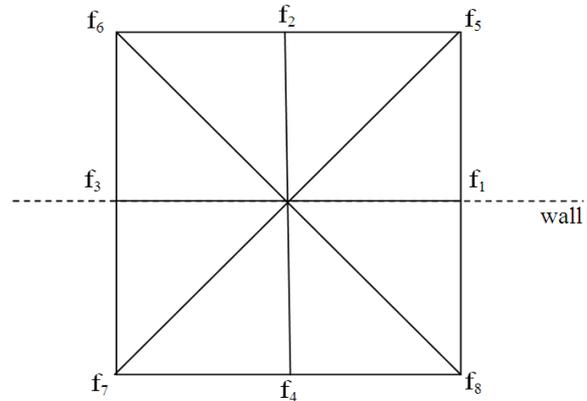
Figure 1. Distribution function for D2Q9 configuration on the upper wall

In order to implement the conservative momentum equations in computational domain, it is required to take the hydrodynamic moments. It consists of two components of momentum (Π_X, Π_Y) and the remaining independent component of the momentum flux (Π_{XXY}). In scheme BC-1, to simulate the zero velocity on the wall, a bounce-back type of boundary condition on the non-equilibrium part of the distribution function is implemented. Figure 1 is presented to explain the boundary condition used in the current study. The south wall is coinciding with the x-axis and is shown by the dotted line in Figure 1. In scheme BC-2, the no-slip and no-flow boundary conditions result in $u_x = u_y = 0$. It necessitates the tangential derivative of the

velocity alongside the wall to disappear at a solid boundary, $\partial u_x / \partial x = 0$. Accordingly, the equations are set as below to obtain the unknown variables in BC-1and BC-2 schemes.

BC-1 : $\qquad \Pi_X = 0 \qquad \Pi_Y = -F_y/2 \qquad \Pi_{XXY} = -F_y/2$

BC-2 : $\qquad \Pi_X = 0 \qquad \Pi_Y = -F_y/2 \qquad \Pi_{XXY} = \rho/3$

$$M = \begin{pmatrix} 1 & 1 & 1 & 1 & 1 & 1 & 1 & 1 & 1 \\ 0 & 1 & 0 & -1 & 0 & 1 & -1 & -1 & 1 \\ 0 & 0 & 1 & 0 & -1 & 1 & 1 & -1 & -1 \\ 0 & 1 & 0 & 1 & 0 & 1 & 1 & 1 & 1 \\ 0 & 0 & 1 & 0 & 1 & 1 & 1 & 1 & 1 \\ 0 & 0 & 0 & 0 & 0 & 1 & -1 & 1 & -1 \\ 0 & 0 & 0 & 0 & 0 & 1 & -1 & -1 & 1 \\ 0 & 0 & 0 & 0 & 0 & 1 & 1 & -1 & -1 \\ 0 & 0 & 0 & 0 & 0 & 1 & 1 & 1 & 1 \end{pmatrix} \qquad (15)$$

By considering the southern boundary and using the above system of equations, we can calculate the unknown distribution function at the south wall. In BC-2, Equations above are employed to determine f2, f5, and f6 as follows.

$$\begin{aligned} f_2 &= f_4 - 2\rho u_y/3 \\ f_5 &= f_7 + (f_1 - f_3)/2 + F_y/4 \\ f_6 &= f_8 - (f_1 - f_3)/2 + F_y/4 \end{aligned} \qquad (16)$$

Li and Tafti [55] defined f_0 after the collision step according to the mass conservation on each lattice node on the wall. During a full lattice Boltzmann method time step, f_0, f_4, f_7, and f_8 leave the domain at the instant t+0, while the fluid particles f_0, f_2, f_5, and f_6 enter the domain at the instant (t+1)-0. The mass conservation at this lattice node requires:

$$\begin{aligned} (f_0)^{(t+1)-0} &= (f_0)^{t+0} + \\ (f_4 + f_7 + f_8)^{t+0} &- (f_2 + f_5 + f_6)^{(t+1)-0} \end{aligned}$$

By using the equations above, f_2, f_5, f_6 and ρ are obtained as below for BC-2.

$$\begin{aligned} f_2 &= f_1 + f_3 + f_4 + 2\times(f_7 + f_8) - \rho/3 - F_y/2 \\ f_5 &= -f_1 - f_8 + \rho/6 \\ f_5 &= -f_3 - f_7 + \rho/6 \\ \rho &= 2(f_0 + f_1 + f_3 + 2\times(f_4 + f_7 + f_8))/(2 + F_y) \end{aligned} \qquad (17)$$

The advantage of the present approach in expressing boundary conditions is that the various components of the force term have been taken into consideration and thus more continuity in values of the distribution function holds on the wall.

3. Description of the Method

Two physical models, Poiseuille and Rayleigh-Benard convection flow, have been investigated. A Poiseuille flow driven by a forcing mechanism is an excellent example versus which the presented models for boundary conditions may be evaluated. That is because the analytical solution for such flow is known. The velocity profile obtained from the Navier-Stokes equations for incompressible Poiseuille flow is as follows.

$$u_y = u_0 \left(1 - \left(\frac{2y}{Ly} \right)^2 \right) \qquad (18)$$

where $u_0 = F_d Ly^2 / (4\rho \upsilon)$, F_d is the driving force and Ly is the channel width. The grid resolutions from $Ly = 8$ to $Ly = 512$ have been tried. The Reynolds number $Re = u_0 Ly / \upsilon$ has been kept constant. Since the kinematic viscosity depends only on τ, the product $u_0 Ly$ needs to remain constant. It means that if the channel width is doubled, u_0 needs to be halved, and thus the forcing F is decreased eightfold. Zero velocity on the top and bottom boundaries is implemented according to boundary condition explained in the previous section. Inlet and outlet boundary conditions along the flow direction are set to be periodic.

Second model is a Rayleigh-Benard convection. A Rayleigh-Benard convection problem may be explained as follows. Consider a volume of fluid between two parallel plates which is initially at rest. The below the surface is heated. By the raise of the temperature difference between upper and bottom surfaces, the gravitational force in the vertical direction grows. Once a certain level of the temperature gradient is reached, any small perturbation tends to turn the stationary conduction status to a convection situation. The schematic diagram of the flow between two parallel plates and the macroscopic boundary conditions are shown in Figure 2. Thermodynamic equilibrium is maintained at the constant temperature T0. T0 is the average of the heated and cooled wall temperatures.
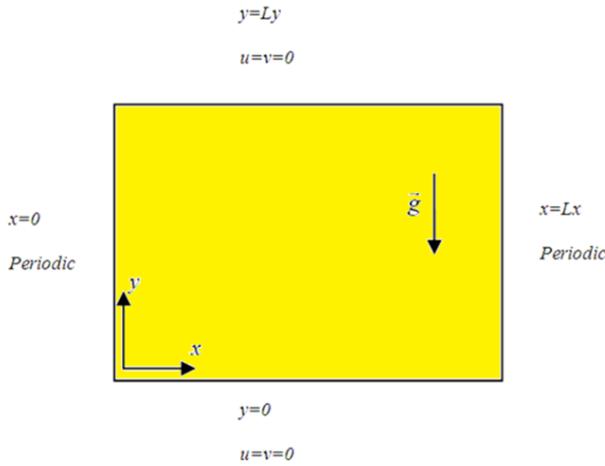
Figure 2. Configuration of natural convection between two plates

The D2Q9 is used to calculate the temperature distribution and velocity profiles. A small disturbance on the density population, similar to what used in some previous studies [46, 61, 62], was considered in the form of a cosine wave with an amplitude of 1×10^{-3}. The Nusselt number and the Rayleigh number are defined as below.

$$Nu = 1 + \frac{\langle u_y T \rangle_x}{\alpha_0 \, \Delta T / L_y}, Ra = \frac{\beta g \left(L y\right)^3 \Delta T}{\upsilon_{avr} \alpha_{avr}} \qquad (19)$$

As reported by Peng et al. [63], the characteristic velocity for natural convection, ($V = \sqrt{g \beta \Delta T L y}$), must be attentively specified to make sure that the lattice Boltzmann equation can still remain within the incompressible regime. The flow incompressibility is maintained when the Mach number (V/c_s) is less than 0.1. Unfortunately, there is no explicit criterion to calculate the characteristic velocity for different natural convection problems. Kao and Yang [46] have explained a method which examines the influence of the characteristic velocity on the critical Rayleigh number at various Prandtl numbers. They also confirmed that the characteristic velocity strongly depends on the Prandtl number. Their method is capable of estimating the range of characteristic velocity for the preservation of incompressibility assumption.

4. Result and Discussion

To evaluate various boundary condition schemes in the present models, Poiseuille Flow has been simulated first. The Rayleigh-Benard convection problem is examined next. The primary and secondary instability of the natural convection have been evaluated under various conditions.

4.1. Poiseuille Flow Case Study

The difference between the velocity predicted by this study and that of the analytical solution, err, is defined by Equation (20).

$$err = \sqrt{\sum_i \left(UN_i - UE_i\right)^2 \Big/ N_n} \qquad (20)$$

where N_n is the number of points, and UE_i and UN_i correspond to the analytical and numerical normalized velocity for the ith node, respectively. Normalization is made by means of the velocity in the center of the channel. The error defined in Equation (20) is expected to decrease with the increase of channel width regardless of the numerical scheme used. As shown in Figure 3, the calculations reveal that the slope of error variations with channel width for both of the boundary condition schemes is about -2. As such, these schemes may be referred to as the second order methods. In terms of the magnitude of error, it is worthwhile to mention that the results of this study provide smaller values of error compared to data of Chen et al. [49] by orders of magnitudes. Note that Chen et al. [49] has applied an extrapolation scheme to model the boundary condition.

The results illustrated in Figure 3 show that the BC-1 boundary conditions lead to a more stable solution in comparison with BC-2. In the latter, some intangible fluctuations in the magnitude of error are observed. The average error may grow, though extremely slowly, with the increase of the number of iterations. At very high numbers of iterations, it may lead to a divergence in the solution. Hence, the BC-1 set of boundary conditions has been chosen for simulation of Rayleigh-Benard convection.

Regarding the body force modeling, it is found that the solutions implementing the Shan and Chen body force modeling [64] and Guo et al. scheme [48] lead to the identical results. In this study, the Scheme of Guo et al. [48] has been selected. Chen et al. [49] used Luo scheme [65] as simplest type of model to simulate the body force.
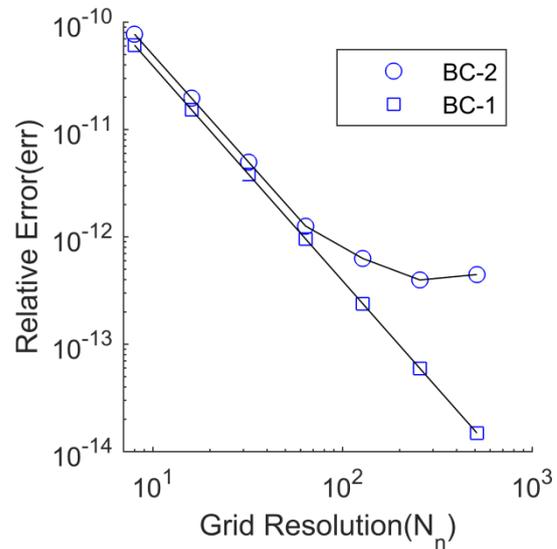
Figure 3 Comparison between the relative error calculated by the BC-1 and BC-2 schemes

4.2. Rayleigh-Benard Convection

The presented thermal lattice Boltzmann method was validated by considering the case of Rayleigh-Benard convection with constant properties. Using the linear stability theory, the exact values of critical wave number and aspect ratio $AR = Lx/Ly$, for constant property Rayleigh–Benard convection are obtained to be 3.117 and 2.016 respectively [66]. The aspect ratio is equal to 2 in the present study. To investigate the grid independency, several different grid sizes, 81x41, 161x81,

321x161 and 641x321 have been examined. The estimated critical Rayleigh numbers at different grid sizes are shown in Table 1. It can be deduced that the increase of the grid size beyond 81x41 does not have a significant effect on the accuracy of the results. The same grid size has been employed in previous studies [44, 46, 67] for 2D channel flow discretized by the square lattice using D2Q9 model. From the results shown in Table 1, it also can be seen that the value of critical Rayleigh number is independent of the Prandtl number.

Table 1 Critical Rayleigh number versus different grid sizes

	81x41	161x81	321x161	641x321
Pr=0.7 (V=0.2915)	1705±1	1706±1	1706±1	1706±1
Pr=5.8 (V=0.1870)	1707±1	1708±1	1708±1	1708±1

A secondary instability, manifested by a time-dependent flow with a single-frequency periodic condition, may occur once the Rayleigh number grows high. The occurrence of such secondary instability is greatly dependent on the Prandtl number. To obtain the actual frequency, the simulation must be started from the static conductive state, i.e. beginning with *Ra<1707*. In the current study, a dimensionless frequency ratio, f^+, is defined as the ratio of the oscillatory time scale (t_p) to the diffusive time scale (Ly^2/α_{avr}) as below.

$$f^+ = \frac{\alpha_{avr} \times t_p}{Ly^2} \tag{21}$$

There is no oscillation for Pr=0.7 until Ra=100,000. Under this condition, four different grid sizes with different Rayleigh numbers are examined. The calculated Nusselt numbers for Ra=50,000 and Ra=100,000 are shown in Table 2, the grid size of 41x81 is not adequate to obtain the required accuracy.

Table 2 Nusselt number calculated by Scheme of Guo and semi-empirical correlation for various Rayleigh numbers with various grids and Pr=0.7

	Nusselt Number	
	Ra=50,000	Ra=100,000
81x41	4.087	4.897
161x81	4.130	4.951
321x161	4.152	4.978
641x321	4.163	4.995
Semi empirical correlation: 1.56×(Ra/Rac)^0.296	4.239	5.205

For Pr=5.8, the results verify the previous findings of Kao and Yang [46] that the flow oscillation starts at Ra≈48,000. As can be observed in Table 3, maximum, minimum and average Nusselt numbers increase with the increment of the number of grids. Meanwhile, by increasing the number of grids, the oscillatory time scale has been decreased. The effect of this reduction in the amount of dimensionless frequency ratio is negligible. Most of

past studies have been used 81x41 grids [44, 46, 67]. It does not mean, however, that such grid size assures the criterion for grid independence of the solution. For instance, Kao and Yang [46] noted that they selected the grid size of 81x41 simply to make their results comparable with the other studies. The data shown in Table 3 states that using 81x41 grids does not lead to adequate accuracy. Based on Table **2** and Table 3, the simulations in the current study for higher Rayleigh number is performed by 641x321 grids. Streamlines and isotherms for the Ra=10^5 and Pr=5.8 are shown in Figure 4 and Figure 5. As can be seen, by marching in time, the vortex center moves in the domain. This movement effect on the isotherm lines and it leads to variation of the nusselt number during the time. When the vortex approaching the wall, the isotherm lines start to close to each other and they make the higher heat transfer coefficient.

5. Conclusion

In this study, using the lattice Boltzmann method, the effects of Prandtl number in the Instability of Rayleigh-Benard convection problem have been investigated. Primary instability is completely independent of Prandtl number and occurs in Ra=1707. As regards, the onset of the secondary instability depend on the Prandtl number and it happens in Ra=4800 for Pr=5.8. Results show that the oscillatory behavior causes the center of the vortex to move in an elliptic manner in the flow field. It is observed that the dimensionless frequency ratio for Ra= 10^5 with Pr=5.8 is around 0.0065.

Table 3 Oscillatory time scale, dimensionless frequency ratio and Nusselt number calculated by Scheme of Guo for Ra=100,000 and Pr=5.8

	$t_p/\Delta t$	f^+	Nu number		
			max	min	Ave.
81x41	1107	0.0067	5.4205	3.4708	4.3929
161x81	1100	0.0067	5.4669	3.5435	4.4576
321x161	1091	0.0066	5.4882	3.5715	4.4810
641x321	1078	0.0065	5.4942	3.5878	4.4966
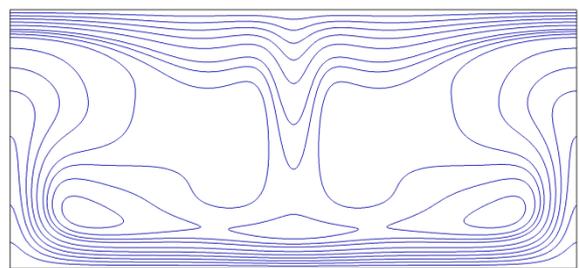
(a)
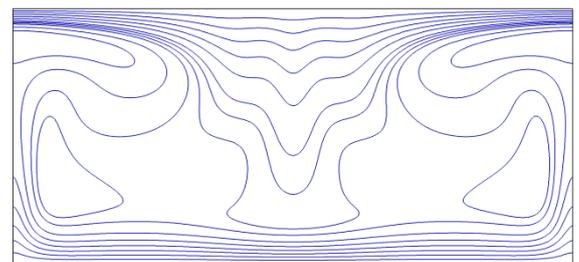
(b)
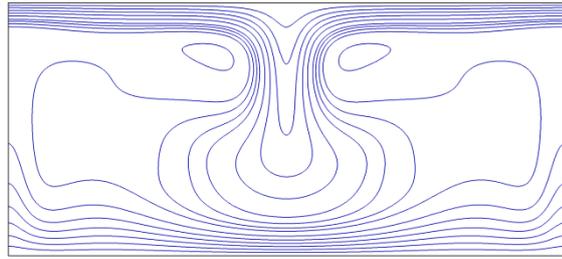
(c)
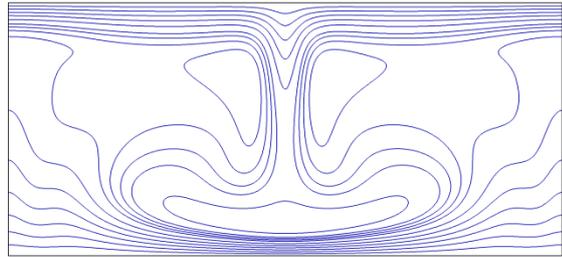
(d)

Figure 4 Streamlines at Ra=100,000 with 641x321 grid sizes calculated by Scheme of Guo (Pr=5.8) in quarter-period steps, i.e. at t= 0 (a), t= tp/4 (b), t=tp/2 (c) and t=3tp/4 (d)
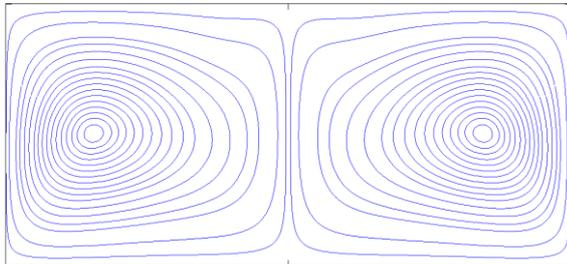
(a)
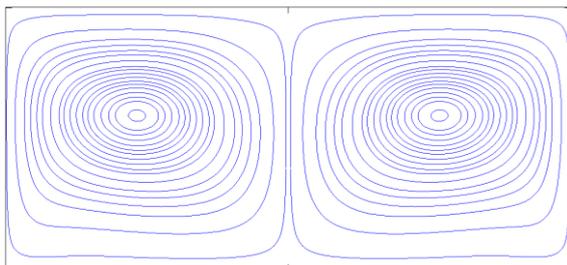
(b)
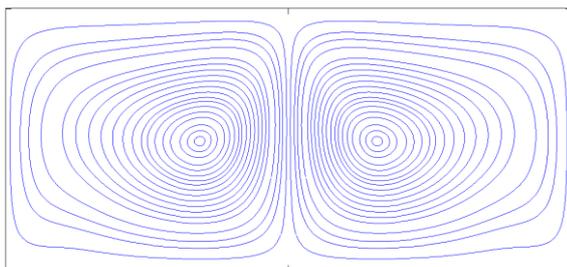
(c)
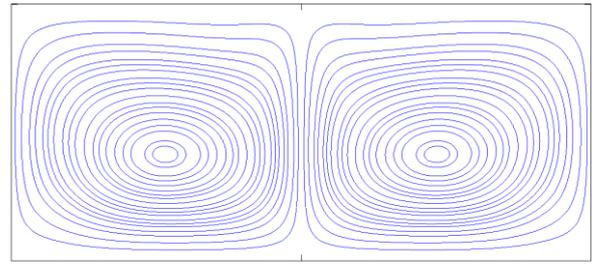
(d)

Figure 5 Temperature contours at Ra=100,000 with 641x321 grid sizes calculated by Scheme of Guo (Pr=5.8) in quarter-period steps, i.e. at t= 0 (a), t= tp/4 (b), t=tp/2 (c) and t=3tp/4 (d)

References

[1]   A. Soloviev, B. Klinger, Open ocean convection, *Elements of Physical Oceanography: A derivative of the Encyclopedia of Ocean Sciences*, pp. 414, 2009.

[2]   M. M. Holland, C. M. Bitz, M. Eby, A. J. Weaver, The role of ice-ocean interactions in the variability of the North Atlantic thermohaline circulation, *Journal of Climate,* Vol. 14, No. 5, pp. 656-675, 2001.

[3]   A. Wirth, B. Barnier, Tilted plumes in numerical convection experiments, *Ocean Model,* Vol. 12, pp. 101-111, 2006.

[4]   D.-J. Yao, J.-R. Chen, W.-T. Ju, Micro–Rayleigh-Bénard convection polymerase chain reaction system, *Journal of Micro/Nanolithography, MEMS, and MOEMS,* Vol. 6, No. 4, pp. 043007-043007-9, 2007.

[5]   N. Agrawal, V. M. Ugaz, A buoyancy-driven compact thermocycler for rapid PCR, *Clinics in laboratory medicine,* Vol. 27, No. 1, pp. 215-223, 2007.

[6]   M. Hennig, D. Braun, Convective polymerase chain reaction around micro immersion heater, *Applied Physics Letters,* Vol. 87, No. 18, pp. 183901, 2005.

[7]   S. Banerjee, A. Mukhopadhyay, S. Sen, R. Ganguly, Natural convection in a bi-heater configuration of passive electronic cooling, *International Journal of Thermal Sciences,* Vol. 47, No. 11, pp. 1516-1527, 2008.

[8]   A. Chaehoi, F. Mailly, L. Latorre, P. Nouet, Experimental and finite-element study of convective accelerometer on CMOS, *Sensors and Actuators A: Physical,* Vol. 132, No. 1, pp. 78-84, 2006.

[9]   Z.-Y. Guo, Z.-X. Li, Size effect on microscale single-phase flow and heat transfer, *International Journal of Heat and Mass Transfer,* Vol. 46, No. 1, pp. 149-159, 2003.

[10]   X. J. Hu, A. Jain, K. E. Goodson, Investigation of the natural convection boundary condition in microfabricated structures, *International Journal of Thermal Sciences,* Vol. 47, No. 7, pp. 820-824, 2008.

[11]   M.-S. Nazari, M. Kayhani, A Comparative Solution of Natural Convection in an Open Cavity using Different Boundary Conditions via Lattice Boltzmann Method, *Journal of Heat and Mass Transfer Research(JHMTR),* Vol. 3, No. 2, pp. 115-129, 2016.

[12]   G. Sobamowo, Analysis of Heat transfer in Porous Fin with Temperature-dependent Thermal Conductivity and Internal Heat Generation using Chebychev Spectral Collocation Method, *Journal of Computational Applied Mechanics*, pp. -, 2017.

[13]   G. C. Rana, R. Chand, V. Sharma, A. Sharda, On the onset of triple-diffusive convection in a layer of nanofluid,

Journal of Computational Applied Mechanics, Vol. 47, No. 1, pp. 67-77, 2016.

[14] G. Ahlers, S. Grossmann, D. Lohse, Heat transfer and large scale dynamics in turbulent Rayleigh-Bénard convection, *Reviews of modern physics,* Vol. 81, No. 2, pp. 503, 2009.

[15] A. Puhl, M. M. Mansour, M. Mareschal, Quantitative comparison of molecular dynamics with hydrodynamics in Rayleigh-Benard convection, *Physical Review A,* Vol. 40, No. 4, pp. 1999, 1989.

[16] E. D. Siggia, High Rayleigh number convection, *Annual review of fluid mechanics,* Vol. 26, No. 1, pp. 137-168, 1994.

[17] G. Freund, W. Pesch, W. Zimmermann, Rayleigh–Bénard convection in the presence of spatial temperature modulations, *Journal of Fluid Mechanics,* Vol. 673, pp. 318-348, 2011.

[18] S. Weiß, G. Seiden, E. Bodenschatz, Pattern formation in spatially forced thermal convection, *New Journal of Physics,* Vol. 14, No. 5, pp. 053010, 2012.

[19] G. Seiden, S. Weiss, J. H. McCoy, W. Pesch, E. Bodenschatz, Pattern forming system in the presence of different symmetry-breaking mechanisms, *Physical review letters,* Vol. 101, No. 21, pp. 214503, 2008.

[20] M. Hossain, J. Floryan, Heat transfer due to natural convection in a periodically heated slot, *Journal of Heat Transfer,* Vol. 135, No. 2, pp. 022503, 2013.

[21] M. Hossain, J. M. Floryan, Instabilities of natural convection in a periodically heated layer, *Journal of Fluid Mechanics,* Vol. 733, pp. 33-67, 2013.

[22] P. Ripesi, L. Biferale, M. Sbragaglia, A. Wirth, Natural convection with mixed insulating and conducting boundary conditions: low-and high-Rayleigh-number regimes, *Journal of Fluid Mechanics,* Vol. 742, pp. 636-663, 2014.

[23] S. Chen, G. D. Doolen, Lattice Boltzmann method for fluid flows, *Annual review of fluid mechanics,* Vol. 30, No. 1, pp. 329-364, 1998.

[24] X. He, L.-S. Luo, A priori derivation of the lattice Boltzmann equation, *Physical Review E,* Vol. 55, No. 6, pp. R6333, 1997.

[25] S. Succi, 2001, *The lattice Boltzmann equation: for fluid dynamics and beyond*, Oxford university press,

[26] D. Yu, R. Mei, L.-S. Luo, W. Shyy, Viscous flow computations with the method of lattice Boltzmann equation, *Progress in Aerospace Sciences,* Vol. 39, No. 5, pp. 329-367, 2003.

[27] A. J. Moghadam, TWO-FLUID ELECTROKINETIC FLOW IN A CIRCULAR MICROCHANNEL (RESEARCH NOTE), *International Journal of Engineering-Transactions A: Basics,* Vol. 29, No. 10, pp. 1469, 2016.

[28] P. Pashaie, M. Jafari, H. Baseri, M. Farhadi, Nusselt number estimation along a wavy wall in an inclined lid-driven cavity using adaptive neuro-fuzzy inference system (ANFIS), *International Journal of Engineering-Transactions A: Basics,* Vol. 26, No. 4, pp. 383, 2012.

[29] M. Varmazyar, M. Bazargan, Development of a thermal lattice Boltzmann method to simulate heat transfer problems with variable thermal conductivity, *International Journal of Heat and Mass Transfer,* Vol. 59, pp. 363-371, 2013.

[30] M. Jafari, M. Farhadi, K. Sedighi, E. Fattahi, Effect of wavy wall on convection heat transfer of water-al2o3 nanofluid in a lid-driven cavity using lattice boltzmann method, *International Journal of Engineering-Transactions A: Basics,* Vol. 25, No. 2, pp. 165, 2012.

[31] H. Ashorynejad, M. Sheikholeslami, E. Fattahi, Lattice boltzmann simulation of nanofluids natural convection heat transfer in concentric annulus, *International Journal*

of Engineering-Transactions B: Applications, Vol. 26, No. 8, pp. 895, 2013.

[32] M. Varmazyar, M. Bazargan, A. Moahmmadi, A. Rahbari, Error Analysis of Thermal Lattice Boltzmann Method in Natural Convection Problems with Varying Fluid Thermal Diffusion Coefficient, *Modares Mechanical Engineering,* Vol. 16, No. 12, pp. 335-344, 2016.

[33] S. Chen, H. Chen, D. Martinez, W. Matthaeus, Lattice Boltzmann model for simulation of magnetohydrodynamics, *Physical Review Letters,* Vol. 67, No. 27, pp. 3776, 1991.

[34] B. M. Riley, J. C. Richard, S. S. Girimaji, Assessment of magnetohydrodynamic lattice Boltzmann schemes in turbulence and rectangular jets, *International Journal of Modern Physics C,* Vol. 19, No. 08, pp. 1211-1220, 2008.

[35] X. He, S. Chen, R. Zhang, A lattice Boltzmann scheme for incompressible multiphase flow and its application in simulation of Rayleigh–Taylor instability, *Journal of Computational Physics,* Vol. 152, No. 2, pp. 642-663, 1999.

[36] T. Inamuro, T. Ogata, S. Tajima, N. Konishi, A lattice Boltzmann method for incompressible two-phase flows with large density differences, *Journal of Computational Physics,* Vol. 198, No. 2, pp. 628-644, 2004.

[37] S. Tilehboni, K. Sedighi, M. Farhadi, E. Fattahi, Lattice Boltzmann simulation of deformation and breakup of a droplet under gravity force using interparticle potential model, *International Journal of Engineering-Transactions A: Basics,* Vol. 26, No. 7, pp. 781, 2013.

[38] M. H. Rahimian, R. Haghani, Four different types of a single drop dripping down a hole under gravity by lattice Boltzmann method, *Journal of Computational Applied Mechanics,* Vol. 47, No. 1, pp. 89-98, 2016.

[39] M. Varmazyar, M. Bazargan, Modeling of Free Convection Heat Transfer to a Supercritical Fluid in a Square Enclosure by the Lattice Boltzmann Method, *Journal of Heat Transfer,* Vol. 133, No. 2, pp. 022501, 2011.

[40] L.-S. Luo, Unified theory of lattice Boltzmann models for nonideal gases, *Physical review letters,* Vol. 81, No. 8, pp. 1618, 1998.

[41] M. Varmazyar, M. Bazargan, Numerical Investigation of the Piston Effect of Supercritical Fluid under Microgravity Conditions Using Lattice Boltzmann Method, *Modares Mechanical Engineering,* Vol. 17, No. 5, pp. 138-146, 2017.

[42] X. Shan, Simulation of Rayleigh-Bénard convection using a lattice Boltzmann method, *Physical Review E,* Vol. 55, No. 3, pp. 2780, 1997.

[43] F. Busse, H. Frick, Square-pattern convection in fluids with strongly temperature-dependent viscosity, *Journal of fluid mechanics,* Vol. 150, pp. 451-465, 1985.

[44] X. He, S. Chen, G. D. Doolen, A novel thermal model for the lattice Boltzmann method in incompressible limit, *Journal of Computational Physics,* Vol. 146, No. 1, pp. 282-300, 1998.

[45] R. Clever, F. Busse, Transition to time-dependent convection, *Journal of Fluid Mechanics,* Vol. 65, No. 04, pp. 625-645, 1974.

[46] P.-H. Kao, R.-J. Yang, Simulating oscillatory flows in Rayleigh–Benard convection using the lattice Boltzmann method, *International Journal of Heat and Mass Transfer,* Vol. 50, No. 17, pp. 3315-3328, 2007.

[47] J. Wang, D. Wang, P. Lallemand, L.-S. Luo, Lattice Boltzmann simulations of thermal convective flows in two dimensions, *Computers & Mathematics with Applications,* Vol. 65, No. 2, pp. 262-286, 2013.

[48] Z. Guo, C. Zheng, B. Shi, Discrete lattice effects on the forcing term in the lattice Boltzmann method, *Physical Review E,* Vol. 65, No. 4, pp. 046308, 2002.

[49] S. Chen, D. Martinez, R. Mei, On boundary conditions in lattice Boltzmann methods, *Physics of Fluids (1994-present),* Vol. 8, No. 9, pp. 2527-2536, 1996.

[50] J. Latt, *Hydrodynamic limit of lattice Boltzmann equations*, Thesis, University of Geneva, 2007.

[51] J. Latt, B. Chopard, O. Malaspinas, M. Deville, A. Michler, Straight velocity boundaries in the lattice Boltzmann method, *Physical Review E,* Vol. 77, No. 5, pp. 056703, 2008.

[52] N. S. Martys, H. Chen, Simulation of multicomponent fluids in complex three-dimensional geometries by the lattice Boltzmann method, *Physical review E,* Vol. 53, No. 1, pp. 743, 1996.

[53] D. R. Noble, S. Chen, J. G. Georgiadis, R. O. Buckius, A consistent hydrodynamic boundary condition for the lattice Boltzmann method, *Physics of Fluids (1994-present),* Vol. 7, No. 1, pp. 203-209, 1995.

[54] P. Skordos, Initial and boundary conditions for the lattice Boltzmann method, *Physical Review E,* Vol. 48, No. 6, pp. 4823, 1993.

[55] S.-M. Li, D. K. Tafti, Near-critical CO_2 liquid–vapor flow in a sub-microchannel. Part I: Mean-field free-energy D2Q9 lattice Boltzmann method, *International Journal of Multiphase Flow,* Vol. 35, No. 8, pp. 725-737, 2009.

[56] R. Allen, T. Reis, A lattice Boltzmann model for natural convection in cavities, *International Journal of Heat and Fluid Flow*, 2013.

[57] S. Bennett, *A lattice Boltzmann model for diffusion of binary gas mixtures*, Thesis, University of Cambridge, 2010.

[58] P. L. Bhatnagar, E. P. Gross, M. Krook, A model for collision processes in gases. I. Small amplitude processes in charged and neutral one-component systems, *Physical review,* Vol. 94, No. 3, pp. 511, 1954.

[59] A. Ladd, R. Verberg, Lattice-Boltzmann simulations of particle-fluid suspensions, *Journal of Statistical Physics,* Vol. 104, No. 5-6, pp. 1191-1251, 2001.

[60] N. S. Martys, J. F. Douglas, Critical properties and phase separation in lattice Boltzmann fluid mixtures, *Physical Review E,* Vol. 63, No. 3, pp. 031205, 2001.

[61] T. Inamuro, M. Yoshino, H. Inoue, R. Mizuno, F. Ogino, A lattice Boltzmann method for a binary miscible fluid mixture and its application to a heat-transfer problem, *Journal of Computational Physics,* Vol. 179, No. 1, pp. 201-215, 2002.

[62] Y. Zhou, R. Zhang, I. Staroselsky, H. Chen, Numerical simulation of laminar and turbulent buoyancy-driven flows using a lattice Boltzmann based algorithm, *International Journal of Heat and Mass Transfer,* Vol. 47, No. 22, pp. 4869-4879, 2004.

[63] Y. Peng, C. Shu, Y. Chew, Simplified thermal lattice Boltzmann model for incompressible thermal flows, *Physical Review E,* Vol. 68, No. 2, pp. 026701, 2003.

[64] X. Shan, H. Chen, Simulation of nonideal gases and gas-liquid phase transitions by the lattice Boltzmann Equation, *Phys. Rev. E. v49 i4*, pp. 2941-2948.

[65] L.-S. Luo, Lattice-gas automata and lattice Boltzmann equations for two-dimensional hydrodynamics, 1993.

[66] W. Reid, D. Harris, Some further results on the Bénard problem, *Physics of Fluids (1958-1988),* Vol. 1, No. 2, pp. 102-110, 1958.

[67] K. Xu, S. H. Lui, Rayleigh-Bénard simulation using the gas-kinetic Bhatnagar-Gross-Krook scheme in the incompressible limit, *Physical Review E,* Vol. 60, No. 1, pp. 464, 1999.